The Impact of Sub-optimal Pulse Sequence Implementations on XTC MRI Measurements

K. Ruppert[1], C-L. Teng[1], I. M. Dregely[2], J. F. Mata[1], T. A. Altes[1], G. W. Miller[1], and J. P. Mugler III[1]
[1]University of Virginia, Charlottesville, VA, United States, [2]University of New Hampshire, Durham, NH, United States

Introduction: Xenon polarization Transfer Contrast (XTC) MRI [1] is a technique that characterizes pulmonary function by acquiring a series of hyperpolarized xenon-129 (HXe129) ventilation images separated by a contrast-generating period. During the latter a series of narrow-bandwidth RF pulses is applied at the resonance frequency for xenon dissolved in lung parenchyma, approximately 200 ppm removed from the xenon gas phase resonance. These pulses partially or fully saturate or even invert the dissolved-phase (DP) magnetization, which, after a certain delay period to permit gas exchange, imprints an additional, exchange-specific decay on the gas-phase (GP) magnetization. Over the years, XTC MRI has been implemented in several different variants that conceptually all measure the same quantities [1-4]. In this work we expand upon the analytical findings by Hrovat et al [5] by presenting numerical results for the impact of specific XTC MRI pulse sequence implementations and inherent limitations on the measured lung-function parameters.

Methods: Using the one-dimensional alveolar wall model described in [2] we simulated the HXe129 gas-phase magnetization in response to simplified XTC MRI pulse sequences in various configurations. Similar to the approach in [5] the initial longitudinal xenon DP magnetization was calculated after the first RF pulse at the DP resonance (for simplification reasons all RF pulses were assumed to be infinitely short and to leave the gas-phase magnetization completely unchanged). The subsequent temporal evolution of the DP magnetization during a delay time (Delay Time 1) was evaluated numerically at 1,000 equidistantly-spaced sampling points across a hypothetic alveolar wall of 5 μm thickness using Eq. 4 in [2]. The first 1,000 terms of the infinite sums were calculated. Additional terms did not significantly contribute to the results any more. It was further assumed that any increase in DP magnetization was associated with an equal but opposite decrease in GP magnetization. Then, the effect of a second RF pulse on the longitudinal DP magnetization was computed followed by the evolution of the DP magnetization during a second delay time (Delay Time 2). This process was repeated 20 times and the change of the GP magnetization after the i-th pulse pair relative to that of the (i-1)th pulse pair was stored. The simulations were performed for Delay Time 1 ranging from 0.01 – 40 ms and for Delay Time 2 set to 100 ms [2], 20 ms or equal to Delay Time 1 [1,3,4]. The GP depolarization as a function of Delay Time 1 was fitted to a mono-exponential recovery curve with an offset (see [2]), which yielded a saturation time constant τ and an asymptotically-approached maximum GP depolarization F_{max}. To investigate the impact of grossly misadjusted XTC MRI pulse sequence parameters we also simulated the impact of xenon DP diffusion constants that were 50% and 75% lower than experimentally determined [2] as an intentional violation of the assumption in the underlying model that τ << Delay Time 2.

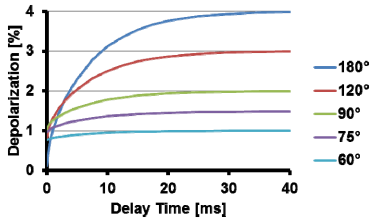

Figure 1. Simulated GP depolarization as function of Delay Time 1 for various flip angles. This represents a near-ideal configuration with a 100 ms Delay Time 2.

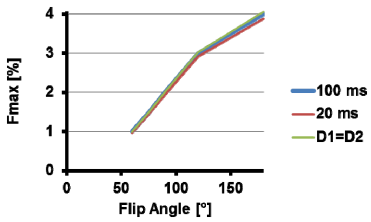

Figure 2. Maximum GP depolarization as a function of flip angle for a Delay Time 2 of 100 ms, 20 ms or equal to Delay Time 1.

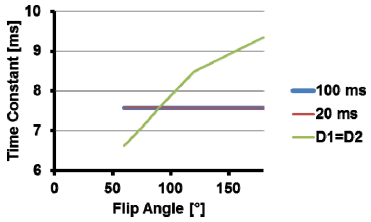

Figure 3. Time constants of the fitted mono-exponential recovery curve (see Fig. 1) as a function of flip angle for a Delay Time 2 of 100 ms, 20 ms or equal to Delay Time 1.

Results and Discussion: Figure 1 depicts the GP depolarization as a function of Delay Time 1 in an ideally-configured (i.e., Delay Time 2 = 100 ms >> τ) XTC MRI sequence with contrast-generating RF pulses of various flip angles. The use of low flip angle RF pulses considerably compresses the dynamic range of the GP depolarization. For the measurement of F_{max} this effect could be overcome by using more RF pulses in the train. However, although τ is the same for all curves in Fig. 1 (not shown), signal-to-noise limitations will make an accurate τ determination with techniques such as MXTC MRI [4] very challenging at low-flip angles. As illustrated in Fig. 2, within the errors of an actual experiment F_{max} can be accurately determined over a wide range of Delay Time 2 values. Nevertheless, as shown in Fig. 3, in a commonly used configuration in which the two delay times are equal [1,3,4] to minimize the acquisition time the error in τ can be substantial except for flip angles around 90°. Thus, it would be preferable to always use a constant Delay Time 2 even if it is too short to allow for the ideally desired complete gas exchange in between RF pulse pairs. Our simulations further indicate that XTC MRI measurements are fairly insensitive to a violation of the model assumption that Delay Time 2 is much larger than τ (not shown). For a diffusion constant 75% lower than measured (i.e., τ would be 4 times larger than anticipated) the errors in F_{max} and τ would not exceed 25% and the erroneous assumption would be clearly apparent in the non-asymptotic depolarization curves.

Conclusion: While technical or physiological constraints may dictate the specifics of a given XTC MRI configuration our findings restrict the usable pulse sequence parameter space that is likely to yield measurement results of acceptable quality. In particular, flip angles below 120° for the contrast-generating RF pulses and / or a non-constant Delay Time 2 should be avoided whenever possible.

References: **[1]** Ruppert K et al. MRM 2000;44:349-357. **[2]** Ruppert K et al. MRM 2004;51:676-687. **[3]** Patz S et al. Acad Rad 2008;15:713-727. **[4]** Dregely IM et al. ISMRM 2010;2554. **[5]** Hrovat MI et al. ISMRM 2010;2556.

Acknowledgements: Supported by NIH grants R01 EB003202 and R01 HL079077, and Siemens Medical Solutions.